Homological analysis of multi-qubit entanglement

Alessandra Di Pierro*,[1] Stefano Mancini†,[2,3] Laleh Memarzadeh‡,[4] and Riccardo Mengoni§[1]

[1]*Department of Informatics, University fo Verona, Strada Le Grazie 15, 37134 Verona, Italy*
[2]*School of Science and Technology, University of Camerino, I-62032 Camerino, Italy*
[3]*INFN-Sezione di Perugia, I-06123 Perugia, Italy*
[4]*Department of Physics, Sharif University of Technology, Teheran, Iran*

We propose the usage of persistent homologies to characterize multipartite entanglement. On a multi-qubit data set we introduce metric-like measures defined in terms of bipartite entanglement and then we derive barcodes. We show that, depending on the distance, they are able to produce different classifications. In one case, it is possible to obtain the standard separability classes. In the other case, a new classification of entangled states of three and four qubits is provided.

PACS numbers: 03.67.Mn, 02.40.Re, 02.70.-c

arXiv:1802.04572v3 [quant-ph] 27 Aug 2018

I. INTRODUCTION

In the last few decades the interest on quantum entanglement has been turned from purely foundational/philosophical aspects to more practical/applicative ones, thanks to quantum information processing. In this setting, the characterization of entanglement is of uppermost importance, although it results a daunting task in multi-partite systems. Many approaches have been developed, based on combinatorics, group theory, geometry, etc. (see e.g. [1] for a review). However, as far as we know, topological approaches have not been taken into consideration up to now.

Persistent homology is nowadays widely used to analyse classical data sets represented in the form of *point cloud* [2]. It is a particular sampling based technique from algebraic topology, originally introduced in [3], aiming at extracting topological information from high dimensional data sets.

A quantum approach to computing persistent homology has been devised in [4] in order to achieve more efficient algorithms for classical data analysis, but vice versa the usage of persistent homologies in the study of quantum data has not been investigated up to now. Here we propose persistent homologies for characterizing multipartite entanglement. On a multi-qubit data set we introduce semi-metrics defined in terms of bipartite entanglement. We then construct on the quantum data set a family of simplicial complexes indexed by a proximity parameter and derive a characterisation of the associated persistent homology by means of barcodes (i.e. a parameterised version of Betti numbers). We consider two different notions of distance and show that they are able to produce different classifications. In one case, it is possible to obtain the known grouping of separability classes. In the other case, a new classification of entangled states of three and four qubits is provided.

*email: alessandra.dipierro@univr.it
†email: stefano.mancini@unicam.it
‡email: memarzadeh@sharif.edu
§email: riccardo.mengoni@univr.it

II. PERSISTENT HOMOLOGY IN A NUTSHELL

Information about topological properties of a topological space X, such as connected components, holes, voids etc., are encoded in the homology groups $\{H_0(X), H_1(X), H_2(X), \ldots\}$ of the space X, where the k^{th} homology group $H_k(X)$ describes the k-dimensional holes in X [5].

In order to capture the global topological features in a data set, the corresponding space must first be represented as a simplicial complex, i.e. as a collection of simple polytopes called simplices [3]. There are different ways for assigning such simplicial complexes to the data points but all methods are based on distances ϵ between pairs of points. For a fixed method, by changing ϵ, different topological features (such as connected components, tunnels, voids etc.) can be observed in the global complex. Hence varying ϵ from small values to sufficiently large ones enables us to find which topological features persist and hence constitute important properties for the given data set. This method of computing multi-scale homological features of the data points is called *persistent homology*. Those features which at some point vanish by changing the parameter ϵ are considered as noise with no particular significance.

Here we focus on the Rips complex[12] to construct simplicial complexes from data points [6]. In the Rips complex, k-simplices correspond to $(k+1)$ points which are pairwise within distance ϵ. By computing topological features for $\epsilon \in (0, \infty)$, we can produce a barcode, i.e. a collection of horizontal lines in a plane where the horizontal axis represents ϵ, while on the vertical axis the homology generators H_k are placed in arbitrary order. Hereafter, a black line in the barcode will indicate a connected component (homology group H_0), a red line will correspond to a hole (homology group H_1) and a blue line will represent a void (homology group H_2).

III. SEMI-METRICS ON QUANTUM DATA SET

Consider a quantum dataset $\mathcal{Q}$ representing a quantum state $|\Psi_n\rangle$ over n qubit as a point cloud. This dataset is such that to each point in $\mathcal{Q}$ is associated a single qubit. Let $E(i,j)$ be

an entanglement monotone [13] between qubit i and j. Our aim is to define a distance on $\mathcal{Q}$ in such a way that the more entangled two qubit are, the closer they are with respect to that distance. This naturally leads to define such a distance as:

$$D(i,j) := [E(i,j)]^{-1}\,, \tag{1}$$

with $D(i,j) = 0$ iff $i = j$. Note that this does not define a proper metric but a semi-metric because the triangle inequality does not hold.

Since $D(i,j)$ only takes into account bipartite entanglement between pairs of qubits and no other form of entanglement, we introduce a variant of $D(i,j)$ that includes bipartite entanglement between any possible pair of subsets containing qubit i and j as:

$$\widetilde{D}(i,j) := \left[E(i,j) + \prod_{S\in\mathcal{P}} E(S\cup\{i\}, \bar{S}\cup\{j\})\right]^{-1}, \tag{2}$$

where S and its complement $\bar{S}$ belong to the power set $\mathcal{P}$ of the set of all qubit indices except i and j, i.e. the power set of $\{1,2,...,n\}\setminus\{i,j\}$.

It is clear that also $\widetilde{D}(i,j)$ is a semi-metric because, likewise $D(i,j)$, it does not satisfy the triangle inequality.

IV. CLASSIFICATION OF THREE QUBIT STATES USING $\widetilde{D}(i,j)$

For three qubits, Equation (2) becomes

$$\widetilde{D}(i,j) = \Big[E(i,j) + E(i,\{j,k\})E(j,\{i,k\})\Big]^{-1} \tag{3}$$

with $i, \neq\ j\ \neq\ k$. By using this distance, we are able to generate barcodes representing generators of homology groups H_0. This allows us to distinguish the following classes of states, reproducing the standard separability classes.

▷ *Product states*
Pure states of this kind are not entangled and can be written as $|\psi_1\rangle|\psi_2\rangle|\psi_3\rangle$ where $|\psi_i\rangle$ is a generic state for qubit i. In this case, whatever labelling i,j,k of the three qubits, we get $E(i,j) = 0\ \forall i,j$ and $E(i,\{j,k\}) = E(j,\{i,k\}) = 0$. This means that $\widetilde{D}(i,j) = \infty$ for every pair of qubits. The point cloud associated with this state is made up of three points placed at infinite distance from each other, hence the corresponding barcode has the form in Figure 1.

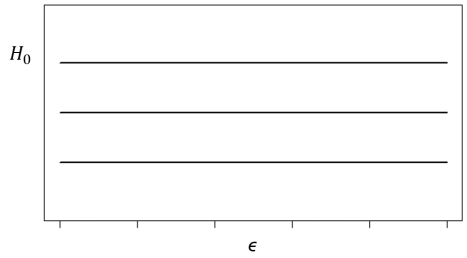


Figure 1: Barcode for three qubit product states.

▷ *Bi-separable states*
Pure states of this kind can be written as $|\psi_i\rangle|\psi_{jk}\rangle$ where $|\psi_{jk}\rangle$ is an entangled states between qubit j and k. In this case we get $E(i,j) = E(i,k) = 0$ and $E(j,k) \neq 0$, while $E(i,\{j,k\}) = 0$ but $E(j,\{i,k\}) \neq 0$ as well as $E(k,\{i,j\}) \neq 0$. This means that $\widetilde{D}(i,j) = \widetilde{D}(i,k) = \infty$ but $\widetilde{D}(j,k) < \infty$. Hence the resulting barcode is as in Figure 2.

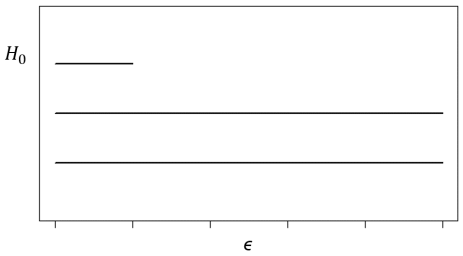


Figure 2: Barcode for three qubit bi-separable states.

▷ *Fully inseparable states*
Pure states of this kind can only be written as $|\psi_{123}\rangle$ i.e. as an entangled three qubit state. States belonging to this class might have $E(i,j) = 0$ or $E(i,j) \neq 0$ for some or all pairs of qubits i and j. However the bipartite entanglement $E(i,\{j,k\})$ and $E(j,\{i,k\})$ always differ from zero $\forall i,j,k$. This means that $0 < \widetilde{D}(i,j) < \infty$, $\forall i,j$. The three points in the point cloud are hence at finite distance from each other and will connect to form a 2-simplex for sufficiently large ϵ.

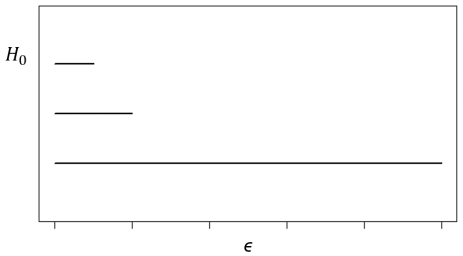


Figure 3: Barcode for three qubit fully inseparable states.

In summary all states in this class give barcodes of the same form of the one depicted in Figure 3, which however may differ in the length of the first two lines depending on the values

of $E(i,j)$, $E(i,\{j,k\})$ and $E(j,\{i,k\})$.

V. CLASSIFICATION OF FOUR QUBIT STATES USING $\widetilde{D}(i,j)$

For four qubit states, Equation (2) becomes

$$\widetilde{D}(i,j) = \Big[E(i,j) + E(i,\{j,k,l\})E(j,\{i,k,l\}) \times E(\{j,l\},\{i,k\})E(\{j,k\},\{i,l\})\Big]^{-1} \tag{4}$$

with $i, \neq j \neq k \neq l$. In a similar way as shown for the three qubit case, it is possible to distinguish between the following classes, each one associated to a different separability class.

▷ *Product states*
Pure states of this kind are fully separable ($|\psi_1\rangle|\psi_2\rangle|\psi_3\rangle|\psi_4\rangle$) and they have associated the barcode in Figure 4;

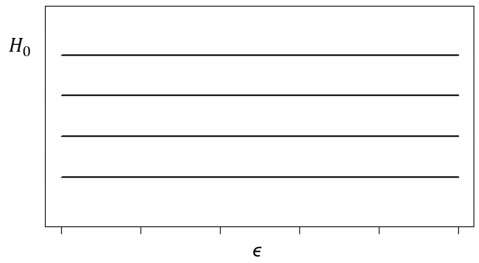


Figure 4: Barcode for product states of four qubits.

▷ *Tri-separable states*
States that are tri-separable (i.e. of the form $|\psi_1\rangle|\psi_2\rangle|\psi_{34}\rangle$) have associated the barcode in Figure 5;

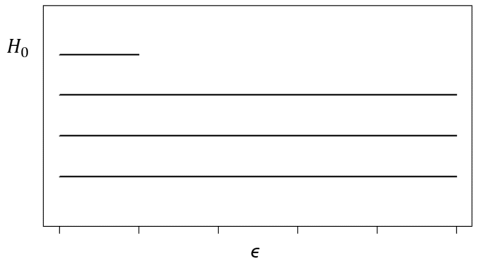


Figure 5: Barcode for four qubit tri-separable states.

▷ *Bi-separable states*
States that are bi-separable (i.e. of the form $|\psi_1\rangle|\psi_{234}\rangle$) have associated the barcode in Figure 6;

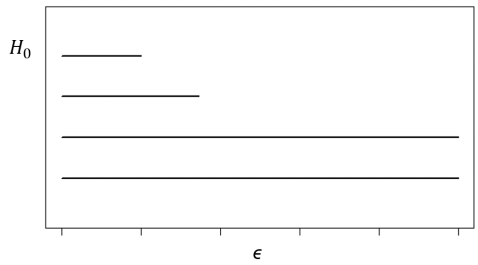


Figure 6: Barcode for four qubit bi-separable states.

▷ *Fully inseparable states*
Such pure states are four-partite entangled (i.e. of the form $|\psi_{1234}\rangle$) and they are all mapped to clouds of four points at finite distance from each another. States of this class have associated the barcodes shown in Figure 7.

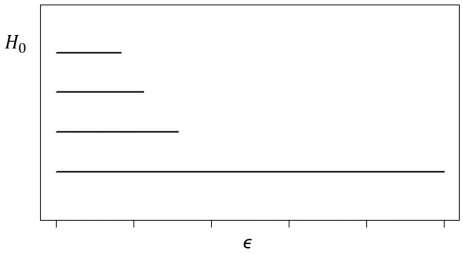


Figure 7: Barcodes for true entangled states of four qubits.

It is worth noticing that, for a generic n-qubit quantum state, barcodes obtained with distance (2) are always able to distinguish between the standard separability classes. The number of bi-partitions needed to calculate $\widetilde{D}(i,j)$ grows with the number of qubits as $2^{n-2}+1$. However, barcodes for the 0-order homology group H_0 are sufficient to recover the standard separability classes, since the number of connected components appearing in the barcode is always upper bounded by the number of qubits n.

VI. CLASSIFICATION OF FULLY INSEPARABLE QUBIT STATES

In the previous section we have provided a classification of multi-qubit states in separability classes. We now concentrate on the fully inseparable set. We will refer to these states also as "true" or "genuine" entangled states. It was shown in [9] that pure states of three-qubit systems showing tripartite entanglement can be further classified into two inequivalent classes under Stochastic Local Operations and Classical Communication (SLOCC). By using the same SLOCC based approach, Verstraete et al. [10] classified generic 4-qubit quantum states in nine different ways. In this section we will address the problem of whether or not a more refined classification of true entangled states is possible by means of barcodes. We will show that this can be done by resorting to the distance D defined by Equation (1).

▷ *Three qubits case*
In the case of genuine three-partite entangled states of three qubits it is possible to recognize the classes listed below. In order to visually distinguish them, we draw the simplicial complex obtained from the point cloud when ϵ is larger than the maximum distance $D(i,j)$ between pairs of qubit.

a) This subclass collects all those states where entanglement between any possible pair of the three qubits gives $E(i,j) = 0$, for all i,j. This implies that each point of our three points cloud is infinitely far away from the others. Hence they generate a barcode that only displays the 0-order homology group H_0, i.e the connected components as shown in Figure 8.

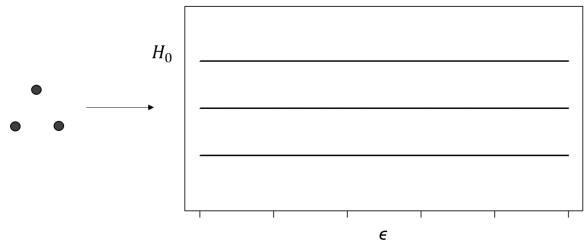


Figure 8: Barcode for three qubit states a)

The state $|GHZ\rangle_3 = \frac{1}{\sqrt{2}}(|000\rangle + |111\rangle)$ can be chosen to be a representative for this class, which exactly corresponds to the GHZ-class of [9].

b) Another class is defined by states where $E(i,j) > 0$, $E(j,k) = 0$ and $E(i,k) = 0$; the associated point cloud is made of three points where the first and the second are at a finite distance, while the third point is at infinite distance from the other two. The barcode shows three different connected components in the interval $\left[0, \frac{1}{E(i,j)}\right]$, while for values grater than $\frac{1}{E(i,j)}$ only two of them persist as shown in Figure 9.

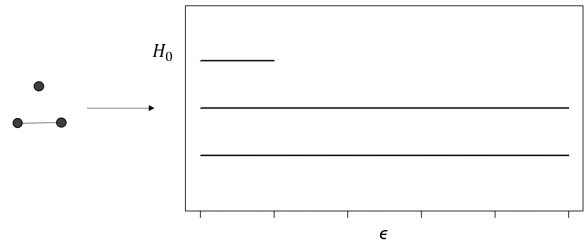


Figure 9: Barcode for three qubit states b)

The state $|\psi_b\rangle_3 = \frac{1}{\sqrt{3}}(|000\rangle + |011\rangle + |111\rangle)$ can be chosen to be a representative for this class. Note that this class constitutes a subset of the W-class found under SLOCC [9].

c) This class contains the following states.
- States with $E(i,j), E(j,k) > 0$ and $E(i,k) = 0$; their associated point cloud is made of three points where the first and the second are at distance $\frac{1}{E(i,j)}$, the second and the third are at distance $\frac{1}{E(j,k)}$, but the first and the third points are at infinite distance. This can be seen in the barcode of Figure 10 where two of the three lines vanishes and only one persists. A representative for this class, with such properties could be the state $|\psi_c\rangle_3 = \frac{1}{\sqrt{3}}(|000\rangle + |001\rangle + |011\rangle + |111\rangle)$.
- States where, at a finite value ϵ^* of $D(i,j)$, the three points get connected one with each other to form a triangular graph that is immediately filled with a 2-simplex. This means that for $\epsilon \geq \epsilon^*$ we are left with only one connected component (the 2-simplex), again shown by the barcode of Figure 10. A representative for this class with such properties could be the state $|W\rangle_3 = \frac{1}{\sqrt{3}}(|100\rangle + |010\rangle + |001\rangle)$.

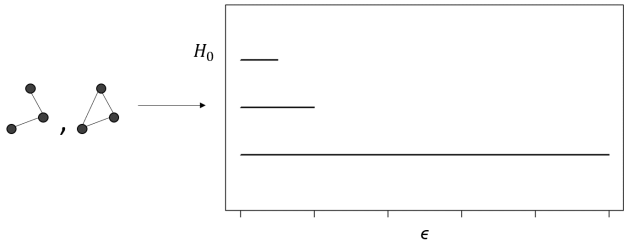


Figure 10: Barcode for three qubit states c)

States of this class constitute another subset of the W-class found using the SLOCC classification. More precisely, the classes b) and c) form a partition of the W-class. In the last section we will show that using another approach to constructing the simplicial complex, it is possible to further distinguish $|W\rangle_3$ from $|\psi_c\rangle_3$ states.

In summary, we have shown that a classification performed using barcodes obtained with distance $D(i,j)$ is able to distinguish 3 different classes of true entangled states of three qubits, hence going beyond the known SLOCC classification.

▷ *Four qubits case*
In the case of four qubit states with genuine four-partite entanglement we can identify six different classes. The results obtained using the distance (1) are summarised in Table I, which refers to barcodes of Figure 11. Also in this case we use the simplicial complex obtained when ϵ is larger than the maximum distance $D(i,j)$ between pairs of qubit in order to visually distinguish different states.

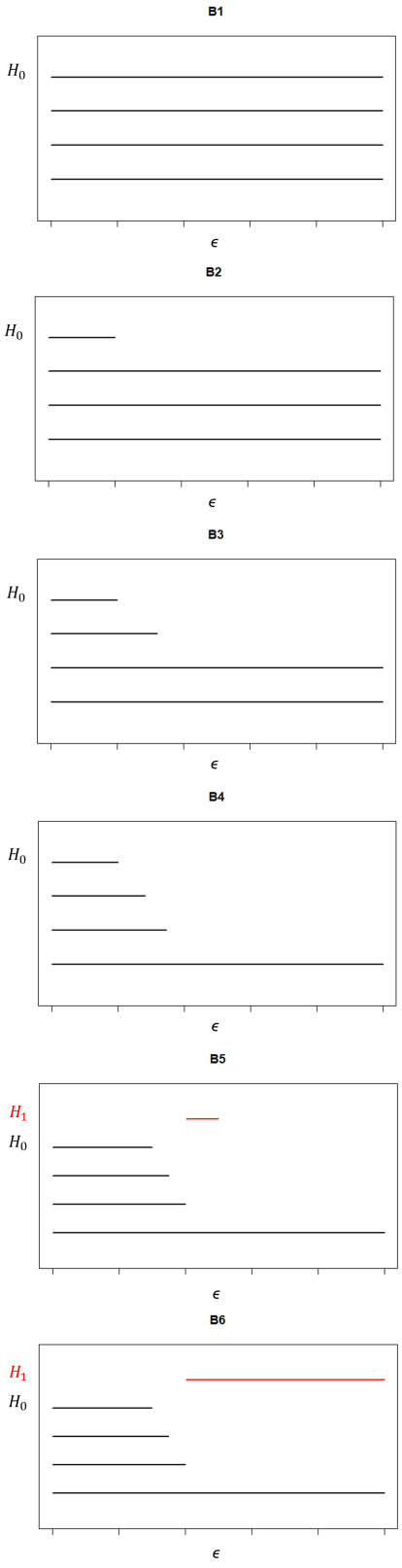


Figure 11: Four qubit barcodes B1-B6

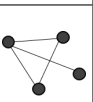
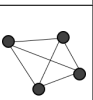
Class	Barcode	Complex	Representative State
a)	B1		$\|GHZ\rangle_4$
b)	B2		$\|B\rangle = \|0000\rangle + \|0111\rangle + \|1101\rangle$
c)	B3		$\|C\rangle = \|0000\rangle + \|0111\rangle + \|1010\rangle + + \|1011\rangle$
	B3		$\|C'\rangle = \|0000\rangle + \|0011\rangle + \|1111\rangle$
	B3		$\|C''\rangle = \|0011\rangle + \|1011\rangle + + \|1101\rangle + \|1110\rangle$
d)	B4		$\|D\rangle = \|0000\rangle + \|0001\rangle + \|1001\rangle + + \|1101\rangle + \|1011\rangle + \|1111\rangle$
	B4		$\|D'\rangle = \|0000\rangle + \|0011\rangle + + \|0111\rangle + \|1110\rangle + \|1111\rangle$
	B4		$\|D''\rangle = \|0000\rangle + \|0011\rangle + + \|0110\rangle + \|0111\rangle + \|1011\rangle$
	B4		$\|D'''\rangle = \|0000\rangle + \|0001\rangle + + \|0011\rangle + \|0101\rangle + \|0111\rangle + + \|1101\rangle$
	B4		$\|W\rangle_4$
e)	B5		$\|E\rangle = 2\|0000\rangle + \|0011\rangle + + \|0110\rangle + \|1001\rangle + \|1100\rangle + + 2\|1111\rangle$
f)	B6		$\|F\rangle = \|0000\rangle + \|0011\rangle + \|1010\rangle + + \|1111\rangle$

Table I: Classification of four-partite entangled states of four qubit.

As we can see from Table I, both classes c) and d) contain states that share the same homology groups although but have different properties (cf. barcodes B3 and B4 in Figure 11). Moreover, it is worth noticing that states like $|W\rangle_4$ and those in class e) are both represented by a 3-simplex for sufficiently large ϵ. The difference is due to the fact that the barcode of states in e) show a hole, i.e. homology group H_1 depicted in red in barcode B5, for a short interval. For large ϵ, this hole gets filled with a 3-simplex and disappears.

As previously said for the three qubit case, we will show in the following section how it is possible to refine also the classification of four qubit entangled states by using a different kind of complex.

VII. RIPS VS ČECH COMPLEX

The Rips complex is closey related to another simplicial complex, called the Čech complex. This is defined on a set of balls and has a simplex for every finite subset of balls with nonempty intersection; thus, while in Rips complexes, k-simplices correspond to $(k+1)$ points which are pairwise within distance ϵ, in Čech complexes k-simplices are determined by $(k+1)$ points whose closed $\epsilon/2$-ball neighborhood have a point of common intersection [8].

By the Čech theorem [7], the Čech complex has the same topological structure as the open sets (ϵ-balls) cover of the point cloud. This is not true for the Rips complex, which is more coarse than the Čech complex. Therefore, the latter is a more powerful tool for classification with respect to Rips. In fact, it is possible to refine the classification of the fully inseparable three qubit states in class c). The reason why this is possible is that in the Čech complex, triangle graphs like the one that appears in the W-state point cloud (Figure 10) are not immediately filled with a 2-simplex. In fact a hole (1-order homology group H_1) appears for a short interval of the values of ϵ before the graph gets filled with the 2-simplex.

Therefore, for the c) class in the three qubit case, barcodes associated to states like $|\psi_c\rangle_3$ remain the same as in Figure 10, the one for the W-like states instead becomes as shown in Figure 12.

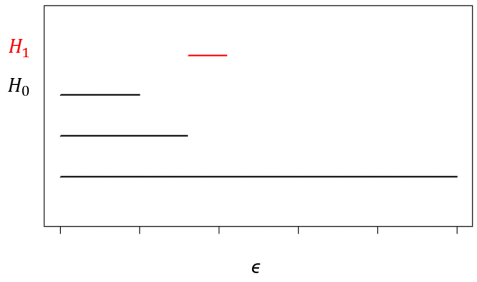


Figure 12: Barcode for W-like states with Čech complex.

Analogously, in the four qubit case, the Čech complex allows us to refine the classification of states in c) and d) classes of Table I. This is shown in Table II with reference to the new barcodes of Figure 13:

Čech barcode	Rips barcode	State
B1	B1	$\|GHZ\rangle_4$
B2	B2	$\|B\rangle$
B3	B3	$\|C\rangle$
B3	B3	$\|C'\rangle$
B4	B4	$\|D\rangle$
B4	B4	$\|D'\rangle$
B5	B4	$\|D''\rangle$
B6	B6	$\|F\rangle$
B7	B3	$\|C''\rangle$
B8	B4	$\|D'''\rangle$
B9	B4	$\|W\rangle_4$
B10	B5	$\|E\rangle$

Table II: Comparison between barcodes obtained from the Rips and Čech complex for fully inseparable states of four qubits

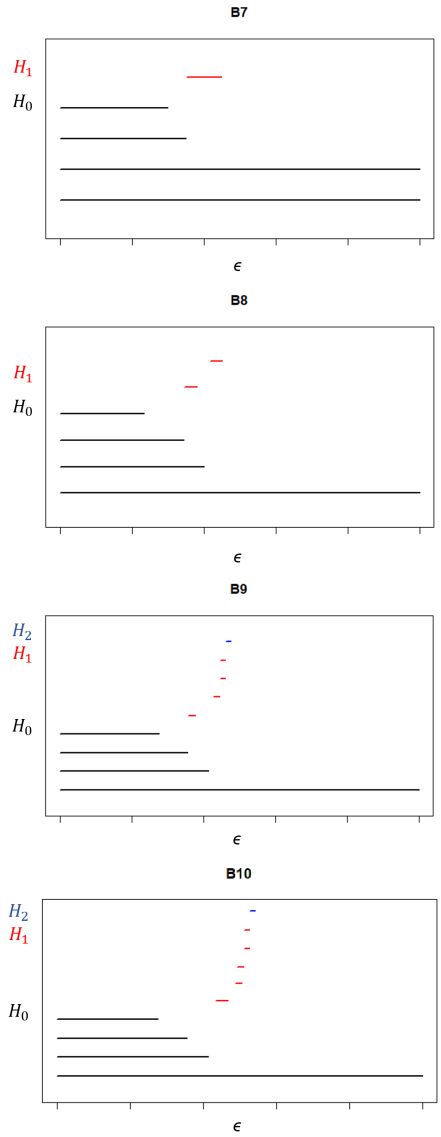


Figure 13: Four qubit barcode B7-B10.

VIII. COMPARISON WITH SLOCC AND GENERALISATION

In [10] it is proposed a classification for pure entangled states of four qubit. This classification is obtained from the orbits generated by SLOCC operations and produces nine classes. Among these nine classes, one is called 'generic' and contains an uncountable number of SLOCC inequivalent classes of states, as shown in [11]. A comparison between the classification based on persistent homology and the one presented in [9] is possible in the three qubit case, as discussed before. However, in the four qubit case, a comparison between our approach and the one in [10] does not allow us to clearly establish a correspondence between classes as in the three qubit case. In order to better understand this, it is useful to consider few specific examples. Consider the class $L_{ab_3} = a(|0000\rangle + |1111\rangle) + \frac{a+b}{2}(|0101\rangle + |1010\rangle) + + \frac{a-b}{2}(|0110\rangle + |1001\rangle) + \frac{i}{\sqrt{2}}(|0001\rangle + |0010\rangle + |0111\rangle + + |1011\rangle)$ defined in [10]. It is easy to check that for the different values of the parameters a and b we obtain the following states:
- for $a = b = 0$, a W-like state with associated barcode B4;
-for $a = 0$ and $b = 1$, a state with barcode B6;
-for $a = b = 1$, a state with barcode B3.
Moreover states belonging to the class $L_{0_{7\oplus\bar{1}}} = |0000\rangle + |1011\rangle + |1101\rangle + |1110\rangle$ have the same barcode of $|GHZ\rangle_4$ which instead belongs to the generic class G_{abcd} for $a = d$ and $b = c = 0$. This makes it impossible to fully characterize the SLOCC classification proposed in [10] in terms of barcodes and vice versa. The SLOCC approach is indeed based on a classification criteria (equivalence with respect to local operations) that are not comparable ours, which are of different nature (the change in the topology of the point cloud formed by the qubit, depending on the pairwise entanglement strength). Therefore the classifications obtained are intrinsically different besides leading to a different number of classes: nine with SLOCC and six (using Rips) or ten (using Čech) with persistent homology. We will nevertheless argue in the following that our approach is mor robust in terms of increasing the number of qubits. In fact, it was shown in [9] that for systems of size $n \geq 4$ there exist infinitely many inequivalent kinds of entanglement under SLOCC and no finite classification is known for states of those sizes. If we restrict to the case of genuine multipartite entangled state of n qubit, it is easy to see that our persistent homology approach always provides a finite number of different classes for any value of n. This is due to the fact that the total number of possible homology groups that can be obtained considering a data set of n point is always finite. The number of possible barcodes B_n obtained with a data set of n points can in fact be bounded from the above as follows

$$B_n < \left(\sum_{e=0}^{\frac{n(n-1)}{2}} G_n(e)\, e! \right) \tag{5}$$

where $G_n(e)$ is the total number of possible graphs with n vertices and e edges, up to permutations of the vertices, and the factorial $e!$ takes into account all the possible ways of constructing $G_n(e)$.

IX. CONCLUSION

We have proposed the use of persistent homologies for the study of multi-partite entanglement. The analysis we have shown, although being a topological analysis gathering as such qualitative information, turns out to be quite powerful. A comparison between the persistent homology classification and known SLOCC classifications [9, 10] highlighted the different nature of these classifications. While on one hand, due to the non local behaviour of entanglement, it is reasonable to use local quantum operations to find equivalence classes, on the other hand, topological properties of entanglement that can be visualised with barcodes are studied. Choosing $\widetilde{D}$ as a distance allows us to represent separability properties of a given state. Distance D instead has been applied to genuinely entangled states to give insights about the topology arising from the bipartite entanglement between pairs of qubits. This analysis allowed us to idenitfy states displaying the same homology groups, providing a new classification.

Looking ahead we plan to apply the presented approach to genuine multipartite entanglement in the case of 5 qubits. There, having no a priori information on entangled states structures we will randomly generate entangled states, then analyse their barcodes, and on the basis of these latter We will single out possible entanglement classes. This method would be efficient when also extended to very large quantum data sets since Eq.(1) implies the calculation of $n(n-1)/2$ correlation measures [in contrast, the classification of all states including partially and fully separable would be of exponential complexity according to Eq.(2)]. Future investigations should also seek true metrics (rather than just semi-metrics) on the quantum data set, since triangle inequality ensures the point cloud to belong to an Euclidean space.

[1] Horodecki R., et al. Rev. Mod. Phys. 812009865.
[2] Carlsson G. and Zomorodian A. Discrete Comput. Geom. 33 2005249.
[3] Edelsbrunner H., Letscher D., and Zomorodian A. Discrete Comput. Geom.28 2002511.
[4] Lloyd S., Garnerone S., and Zanardi P. arXiv:1408.3106 [quant-ph] 2014.
[5] Hatcher, A. Cambridge University Press.2002.
[6] Carlsson, E. et al. Int. J. Comput. Geom. Appl.162006291.
[7] Borsuk K. Fundamenta Mathematicae35(1):217–2341948.
[8] Ghrist, R. Bulletin of the American Mathematical Society, Vol. 452008

[9] Dur W., Vidal G., and Cirac J. I. Phys. Rev. A 62, 0623142000
[10] Verstraete F., Dehaene J., De Moor B., and Verschelde H. Phys. Rev. A 65, 0521122002
[11] G. Gour, N. R. Wallach Journal of Mathematical Physics 51, 112201 2010
[12] Most commonly known as Vietoris-Rips complex, here we will call it Rips complex for the sake of brevity.
[13] Different monotones would produce barcodes with the same homology groups generators, up to sliding or stretching/contraction of the bars.